

CORRELATING THERMAL INERTIA AND OLIVINE ABUNDANCE ON MARS WITH THEMIS.

R.D. Hanna¹ and V.E. Hamilton², ¹Jackson School of Geological Sciences, University of Texas, Austin, TX, 78712 (romy@jsg.utexas.edu), ²Southwest Research Institute, 1050 Walnut St., Suite 300, Boulder, CO 80302 (hamilton@boulder.swri.edu)

Introduction: Bandfield et al. [1] proposed that aqueous alteration has contributed to the formation of soils on Mars, most notably resulting in the chemical alteration of olivine leading to sediments that are olivine-poor relative to the bedrock from which they were derived [1]. If this is indeed true, there should be a positive correlation between olivine abundance and particle size in areas where olivine-bearing materials are found. Using thermal inertia as a proxy for particle size, [1] and [2] presented THEMIS imagery that qualitatively supported this relationship, arguing that chemical weathering of olivine occurs on a global scale on Mars.

We are currently investigating this proposed correlation between olivine content and thermal inertia using a more rigorous, quantitative approach. Our investigations of several olivine-rich regions using TES data found no evidence for a positive correlation between olivine and thermal inertia at the $\sim 3 \times 6$ km resolution of that instrument [3-4]. We hypothesized that the large spatial scale of TES data hid complicated local geological relationships between high and low-olivine abundance materials, precluding a direct positive correlation between olivine content and thermal inertia. To test this hypothesis as well as to quantitatively confirm the findings of [1-2], we have begun to investigate these regions at a higher spatial resolution using thermal inertia and olivine abundance derived from THEMIS data.

Data and Methods: For this study we used data from the Mars Global Surveyor Thermal Emission Spectrometer (TES) and 2001 Mars Odyssey Thermal Emission Imaging System (THEMIS). In each region we chose at least one set of overlapping daytime and nighttime THEMIS images for analysis. We selected warm (average IR surface temperature ≥ 240 K) daytime images with strong evidence of olivine-bearing materials as evidenced by their distinctive magenta color in an 8-7-5 decorrelation stretched (DCS) image [5] for compositional analysis. We selected THEMIS nighttime images to maximize the area of overlap with the olivine-bearing region in the daytime images.

We calculated thermal inertia from the THEMIS nighttime images on a per-pixel basis using the observed surface temperature as a single-temperature input to the KRC thermal model [6], similar to the method of [1]. We obtained olivine abundance from linear least squares fitting of our atmospherically

corrected daytime THEMIS images [1, 7]. The atmospheric correction is described in detail by [7] and consists of selecting a spectrally (compositionally) homogenous area in the image as a training region. We derive a surface spectrum for the region by linearly modeling an appropriate TES spectrum (typically an average of 4-6 pixels, see [4] for selection criteria), using it to extract the atmospheric spectral shape and subtracting this from the rest of the THEMIS image. As discussed by [7], this correction is only appropriate over areas of similar elevation and surface temperatures.

We used a non-negative linear least squares (NNLS) algorithm [8] to model the surface spectrum of THEMIS bands 3-9 [7]. We ran several trials using different combinations of 4-5 end-members and evaluated the results by examining the reported RMS errors and spatial consistency with expected spectral (compositional) units visible in various DCS images. In addition to a blackbody, our other end-members included an atmospheric water ice spectral shape (to account for variable water ice across the image) [9], Surface Types 1 and 2 [10], high albedo surface dust [11], the TES-derived training region surface spectrum, an olivine-bearing basalt [12], and several olivine mineral laboratory spectra [13-14].

Initial Results: The first region we are investigating is the olivine-rich area of southern Isidis. The set of overlapping THEMIS images presented here is the same pair presented by [1] (I19050003 and I01395005). The derived thermal inertia is shown in Figure 1. The compositional results using an end-member set similar to [1] (TES-derived surface, surface dust, and an olivine basalt) are shown in Figure 1, and olivine content vs. thermal inertia is plotted in Figure 2. The distribution and concentration of the three units is broadly similar to [1], although we model more dust in the same areas where olivine is found. We agree that areas with significant olivine appear to have higher thermal inertia. However, Figure 2 indicates that there is no direct correlation between olivine abundance and thermal inertia.

The change in topography across the area shown in these images is quite pronounced, with a range in MOLA elevation from -4460 to -912 m. Because the atmospheric correction is only valid for a limited elevation range, we examined the effect of limiting the NNLS model results to within 500 meters and 1000 meters of the average elevation of the training

region (Fig. 3). We did not observe a marked improvement in the correlation between thermal inertia and olivine basalt abundance.

Although various other end-member set combinations for the NNLS model resulted in slightly different concentrations and distributions of the phases within the area, none of these attempts resulted in a quantitatively positive correlation between thermal inertia and olivine (-bearing rock) content. We did find that including a water ice spectral shape in the end-member library significantly decreased the modeled dust and increased the modeled olivine content, in addition to returning lower RMS errors (Fig. 4). This suggests our atmospheric correction in the area of highest olivine is not ideal and requires more investigation.

Conclusions and Future Work: To date we do not see any correlations between THEMIS-derived thermal inertia and olivine content in the Isidis area. We will investigate if disparate surface temperatures are complicating the atmospheric correction and thus the NNLS model results. We are also looking into further limiting the results to areas that are geologically related, to ensure that the lower inertia materials surveyed are actually derived from the higher inertia materials present in the scene. Finally, we plan to analyze several other olivine-bearing regions for correlation relationships between olivine content and thermal inertia at the THEMIS scale.

References: [1] Bandfield, J.L. et al. (2011), *Icarus*, 211, 157-171 [2] Bandfield, J.L. et al. (2008) *Geology*, 36(7), 579-582 [3] Hamilton, V.E. et al. (2010), LPSC XLI, abs #2239 [4] Hanna, R.D. and Hamilton, V.E. (2013) LPSC XLIV, abs #2235.

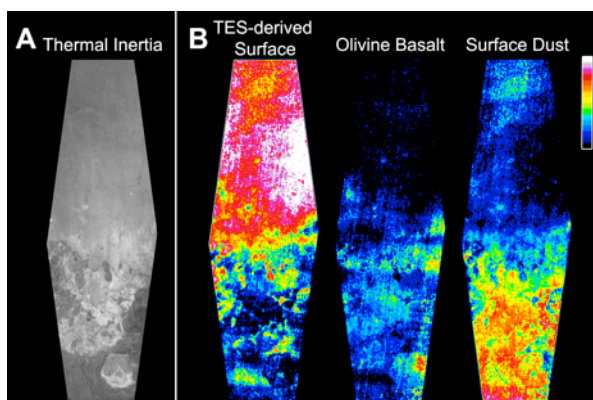


Figure 1. A) Thermal inertia derived from THEMIS nighttime image I19050003, cropped to overlap area with daytime image in (B). B) Spectral end-member maps (concentration color scale from 0 to 100) from NNLS model of I01395005. Images cropped to overlap area with (A). RMS errors <0.0137 in emissivity.

[5] Hamilton, V.E., and Christensen, P.R. (2005) *Geology*, 33, 433-436 [6] Kieffer, H.H. (2013) *JGR*, 118, 3, 451-470 [7] Bandfield, J.L. et al. (2004) *JGR*, 109, doi:10.1029/2004JE002289 [8] Rogers, A.D. and Aharonson, O. (2008) *JGR*, 113 doi:10.1029/2007JE002995 [9] Bandfield, J.L. et al. (2000) *JGR*, 105, 9573-9588 [10] Bandfield, J.L. et al. (2000) *Science*, 287, 5458, 1626-1630 [11] Bandfield, J.L. and Smith, M.D. (2003) *Icarus*, 161, 1, 47-65 [12] Hamilton, V. E. and Ruff, S. W. (2012) *Icarus*, 218, 2, 917-949 [13] Koeppen, W. C. and Hamilton, V. E. (2008) *JGR*, 113, doi:10.1029/2007JE002984 [14] Hamilton, V.E. (2010) *Chemie der Erde*, 70, 1, 7-33.

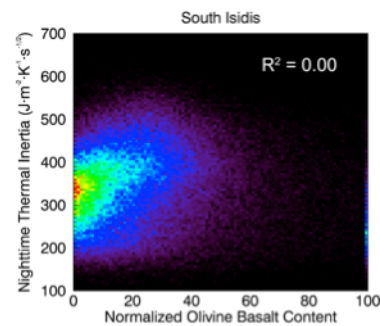


Figure 2. Normalized olivine basalt content versus nighttime thermal inertia derived from THEMIS images in Fig. 1.

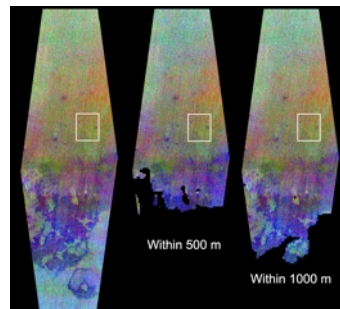


Figure 3. Atmosphericly corrected emissivity image I01395005, cropped to area of overlap with I1905003. Center and right images limited to indicated range beyond average elevation of the training region (white box).

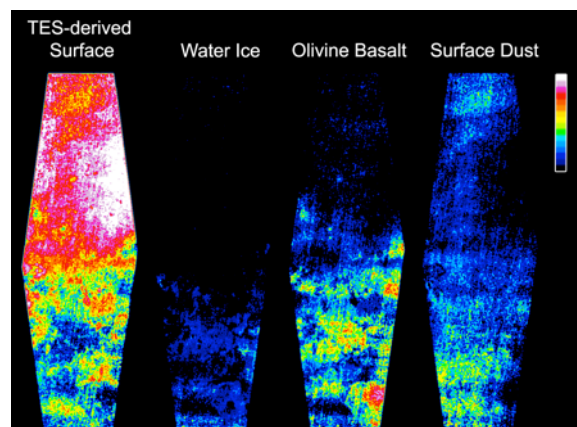


Figure 4. Spectral end-member maps (concentration color scale from 0 to 100) from NNLS model of I01395005. Images cropped to overlap area with nighttime image I19050003. RMS errors <0.0115 in emissivity.